Surface effects in the energy loss of ions passing through a thin foil

J. Osma
Departamento de Física de Materiales, Facultad de Ciencias Químicas, Universidad del País Vasco/Euskal Herriko Unibertsitatea, Apartado 1072, 20080, San Sebastián, Spain

F. J. García de Abajo
Departamento de Ciencias de la Computación e Inteligencia Artificial, Facultad de Informática, Universidad del País Vasco/Euskal Herriko Unibertsitatea, Apartado 649, 20080, San Sebastián, Spain

(Received 15 April 1997)

The role of surface plasmon excitation in the interaction of ions passing through thin films has been studied in both the Bloch hydrodynamic approximation and the local response approach for projectile velocities above the maximum of the stopping power curve. The effect of the surface is found to be much weaker when the dispersion of the modes is taken into consideration than in the case of nondispersive media, though qualitatively the main features of the hydrodynamic approach resemble those of the local one. A generalization of the Bothe-Landau convolution formula for the loss probability distribution is derived to take into account the scattering due to the surface. The effects of the surface in the energy-loss spectra are discussed. A comparison with experiment is given. [S1050-2947(97)05709-0]

PACS number(s): 34.50.Bw

I. INTRODUCTION

Electron-energy-loss spectroscopy and ion-energy-loss spectroscopy have been revealed as important probes of the dielectric response of solids and the intrinsic statistical nature of the particle penetrating phenomena. The advent of new techniques for producing mesoscopic structures such as ultrathin films of a small number of atomic monolayers has renewed the interest in the dependence of the energy deposition process on the target system size. Since the pioneering work of Ritchie [1] on the stopping power experienced by fast electrons crossing a nondispersive plasma slab, much attention has been paid to characterize the response of a thin film. Takimoto [2] gave a detailed study of the plasmon excitation by charged particles outside a metal slab within a nondispersive approach. A Hamiltonian description for a thin foil was considered by Sunjic and Lucas [3]. Further study of the response of a slab has been done within the infinite-barrier model [4,5], with a finite barrier for the surface potential [3] and including self-consistency in the metal electron states [6]. An extension of Ritchie's early work including nonlocal effects in the response of the medium has been carried out by Gumbs and Horing [7] in the random-phase approximation (RPA) and assuming specular reflection of electrons at the slab surfaces. The formation of the wake potential in thin foils was studied within the hydrodynamic approach by García de Abajo and Echenique [8]. This approach was also used by Dorado, Crawford, and Flores [9] to discuss how nonlinear effects associated with plasmon excitations modify the wake and the stopping power in the bulk. More recently, Apell *et al.* [10] showed that the bulk stopping cross section is linear in the inverse of the number of atomic layers.

The energy-loss spectra of charged particles are characterized by pure statistical magnitudes such as the stopping power (mean energy loss per unit length) and the straggling (fluctuation). Nevertheless, this is only true for Gaussian spectra that occur for long path lengths. In fact, when decreasing the thickness of the films, non-Gaussian-like shapes appear due to single-collision-like events. The statistical nature of the energy-loss has been studied by Bohr [11] and Landau [12]. More recently, Sigmund [13,14] developed a theory for the stopping and straggling of charged particles in the presence of charge exchange. This work was extended to include higher moments of the energy-loss distribution and transients by Närmann and Sigmund [15].

In the present paper the surface effect in the energy loss due to the excitation of surface plasmon modes is calculated for thin films within a hydrodynamical approach and its implications in the loss spectra are studied using a Bothe-Landau formula generalized to inhomogeneous media such as surfaces. This formula is used beyond the conventional diffusion approximation, allowing one to study the evolution of the loss spectra as the charged projectile approaches, crosses, and leaves the slab. The effects of changes in the projectile charge state as electron capture and loss are neglected here (this is an approximation valid for large velocities). Atomic units (a.u.) will be used throughout this work, unless stated otherwise.

II. RESPONSE MODEL FOR THE SLAB

The presence of a moving charged particle in the proximity of a slab modifies the charge distribution in the material. The resulting induced potential is of relevance in the dynamical evolution of the particle [16–18]. It leads to a retarding force (though when the projectile approaches the slab, the image acceleration takes place), which makes the particle lose energy.

We will first describe the response of the solid foil within the hydrodynamic model in the linear approximation. The dispersion introduced by this approach permits one to describe properly the coupling of charged particles with both bulk and surface collective modes for velocities just above

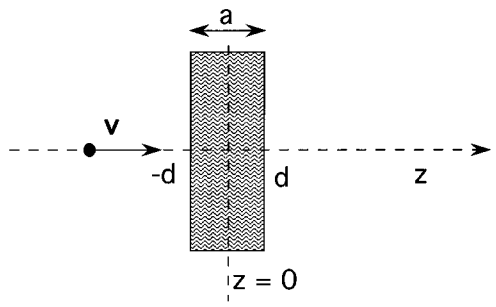

FIG. 1. Geometrical configuration under investigation. The interfaces at $z=-d$ and $z=d$ are of infinite extent.

the maximum of the stopping power curve, where processes of charge exchange do not contribute significantly.

For the sake of comparison, the high-velocity limit is considered, assuming a nondispersive medium. The slab has been chosen to be located between $z=-d$ and d, i.e., the thickness is $a=2d$, and since the external point charge Z_1 is moving perpendicularly to the slab with velocity v crossing its center at $t=0$, the external density is $\rho^e(\mathbf{r})=Z_1\delta(\mathbf{R})\delta(z-vt)$. A schematic of the situation can be seen in Fig. 1.

A. Hydrodynamical approach

In this model, the solid is approximated as a bounded electron gas embedded in a rigid positive background. The electron-gas density n and the velocity potential ψ satisfy the Bloch equations [19] inside the medium, while the scalar electric potential ϕ satisfies the Poisson equation. In the linear-response approximation, the set of equations that n, ψ, and ϕ satisfy when an external charge density ρ^e perturbs the slab reads

$$\begin{aligned}\gamma\psi+\partial\psi/\partial t&=-\phi+\beta^2 n/n_0,\\ \partial n/\partial t&=n_0\nabla^2\psi,\\ \nabla^2\phi&=4\pi(n-\rho^e),\end{aligned}\tag{1}$$

where n_0 is the unperturbed electron density, assumed to be constant throughout the solid. β is the velocity of propagation of the disturbances in the electron gas, which in our case has been chosen as the mean velocity in the Fermi electron gas ($\beta=\sqrt{3/5}v_F$, with v_F the Fermi velocity) and γ is the electron damping rate.

The potential is fixed by the boundary conditions. These are the vanishing of the electron velocity and the continuity of the scalar potential and the electric field at the boundary edges of the slab. The first condition leads to a steplike density profile at the surface. The electron density is zero in the vacuum. The underlying assumption in this model is that the interference between the outgoing and reflected components of the solid electron wave functions is neglected. Therefore, the results given by the well-known specular reflection model [20] are recovered when the thickness of the slab is taken to be infinite [21].

In Fourier-transform space

$$f(\mathbf{r},t)=\int\frac{d\mathbf{Q}}{(2\pi)^2}\int\frac{d\omega}{2\pi}e^{i(\mathbf{Q}\cdot\mathbf{R}-\omega t)}f(\mathbf{Q},z,\omega)$$

the set of equations (1) can be solved for both the velocity and electric potentials. One finds [8]

$$\phi(\mathbf{Q},z,\omega)=\begin{cases}\phi_0(\mathbf{Q},z,\omega)+\omega_p^2[A_-e^{-(d-z)\Lambda}+A_+e^{-(d+z)\Lambda}]-\omega(\omega+i\gamma)[B_-e^{-(d-z)Q}+B_+e^{-(d+z)Q}], & |z|\leqslant d,\\ C_-e^{Q(d+z)}+\dfrac{4\pi e^{i\omega z/v}}{v\tilde{k}^2}, & z\leqslant -d\\ C_+e^{Q(d-z)}+\dfrac{4\pi e^{i\omega z/v}}{v\tilde{k}^2}, & z\geqslant -d\end{cases}\tag{2}$$

for the scalar potential and

$$\psi(\mathbf{Q},z,\omega)=\psi_0(\mathbf{Q},z,\omega)+i\omega[-A_-e^{-(d-z)\Lambda}-A_+e^{-(d+z)\Lambda}+B_-e^{-(d-z)Q}+B_+e^{-(d+z)Q}],$$

with $|z|\leqslant d$, for the velocity potential. $A_\pm$, $B_\pm$ and $C_\pm$ are constants depending on $(\mathbf{Q},\omega)$ that are obtained by imposing the boundary conditions. Moreover,

$$\phi_0(\mathbf{Q},z,\omega)=\Delta[\beta^2\tilde{k}^2-\omega(\omega+i\gamma)]e^{i\omega z/v},$$

$$\psi_0(\mathbf{Q},z,\omega)=\Delta i\gamma\omega e^{i\omega z/v},$$

where we have defined

$$\Lambda(Q,\omega)=\frac{1}{\beta}[\omega_p^2+\beta^2Q^2-\omega(\omega+i\gamma)]^{1/2}$$

and

$$\tilde{k}^2=Q^2+(\omega/v)^2,\quad \Delta=\frac{4\pi}{\tilde{k}^2v}\frac{Z_1}{\beta^2\Lambda^2(\tilde{k},\omega)}.$$

$\mathbf{Q}$ is the surface parallel component of the total momentum transfer $\tilde{k}$ and ω_p is the bulk plasma frequency. The first term in ϕ inside the slab is precisely the bulk potential. The remaining terms account for the surface induced potential. The induced potential is obtained from the total potential by subtracting the external potential:

$$\phi^{ind}(\mathbf{Q},z,\omega)=\phi(\mathbf{Q},z,\omega)-\frac{4\pi Z_1 e^{i\omega z/v}}{v\tilde{k}^2}. \tag{3}$$

The bulk term of the induced potential can be expressed in terms of the dielectric bulk response function $\epsilon(\mathbf{q},\omega)$ as

$$\phi^{ind}_{bulk}(\mathbf{Q},z,\omega)=\phi_0(\mathbf{Q},z,\omega)-\frac{4\pi Z_1 e^{i\omega z/v}}{v\tilde{k}^2}$$
$$=\frac{4\pi Z_1}{v\tilde{k}^2}\left[\frac{1}{\epsilon(\tilde{k},\omega)}-1\right]e^{i\omega z/v},$$

keeping in mind that the bulk response function in the hydrodynamic approach takes the form

$$\epsilon(q,\omega)=1+\frac{\omega_p^2}{\beta^2 q^2-\omega(\omega+i\gamma)}. \tag{4}$$

Following previous authors [22], the rate of energy loss per unit time for a charge Z_1 moving with spatial coordinates $\mathbf{r}(t)$ is given, in terms of its induced potential, by

$$w(t)=Z_1\mathbf{v}\cdot\nabla\phi^{ind}(\mathbf{r},t)|_{\mathbf{r}=\mathbf{r}(t)}=w_{cons}(t)+w_{diss}(t).$$

This rate has two contributions [23], one conservative and the other dissipative:

$$w_{cons}(t)=Z_1\frac{d\phi^{ind}}{dt}(\mathbf{r},t)|_{\mathbf{r}=\mathbf{r}_{Z_1}(t)}$$

and

$$w_{diss}(t)=-Z_1\frac{\partial\phi^{ind}}{\partial t}(\mathbf{r},t)|_{\mathbf{r}=\mathbf{r}_{Z_1}(t)},$$

respectively. Since the polarization of the medium and, consequently, the induced potential vanish when $t=\pm\infty$, the total energy loss suffered by the projectile is entirely due to the dissipation taking place by excitation of the electronic modes of the slab, that is,

$$\Delta E=\int_{-\infty}^{\infty}dt\,w_{diss}(t)$$
$$=\int_0^{\infty}d\omega\,\omega P(\omega)=\int_0^{\infty}d\omega\,\omega\int_{-\infty}^{\infty}dt\,P(\omega,t).$$

$P(\omega,t)$ is the probability per unit time of losing energy ω: the projectile undergoes an energy loss between ω and $\omega+d\omega$ in the interval t and $t+dt$ with probability $P(\omega,t)dtd\omega$. The dependence on t has to be understood as $\mathbf{r}=\mathbf{r}(t)$ and thus $P(\omega,t)$ makes sense only for the especified trajectory $\mathbf{r}=\mathbf{r}(t)$. Since the formalism used here to describe the response of the medium is causal [see Eqs. (1) and (4)] the loss probability at t only depends on the past history of the trajectory traveled by the projectile. Using the induced potential given by Eq. (2) together with Eq. (3), the time-dependent loss probability is found to be

$$P(\omega,t)=-2Z_1\int\frac{d\mathbf{Q}}{(2\pi)^3}\mathrm{Im}\{e^{-i[\omega t-\mathbf{Q}\cdot\mathbf{R}(t)]}\phi^{ind}(\mathbf{Q},z(t),\omega)\}. \tag{5}$$

Integrating along the whole trajectory, the bulk energy loss reduces to

$$\Delta E_{bulk}=\int_0^{\infty}d\omega\,\omega P_{bulk}(\omega), \tag{6}$$

where

$$P_{bulk}(\omega)=\frac{4aZ_1^2}{v^2}\int\frac{d\mathbf{Q}}{(2\pi)^2}\frac{1}{\tilde{k}^2}\mathrm{Im}\left[\frac{-1}{\epsilon(\tilde{k},\omega)}\right], \tag{7}$$

while the surface energy loss reads

$$\Delta E_{surf}=\int_0^{\infty}d\omega\,\omega P_{surf}(\omega), \tag{8}$$

where

$$P_{surf}(\omega)=\frac{Z_1}{\pi}\int\frac{d\mathbf{Q}}{(2\pi)^2}\mathrm{Im}\left\{\omega_p^2\left[\frac{A_-(e^{i\omega d/v}e^{-2\Lambda d}-e^{-i\omega d/v})}{\Lambda v-i\omega}\right.\right.$$
$$\left.+\frac{A_+(e^{-i\omega d/v}e^{-2\Lambda d}-e^{i\omega d/v})}{\Lambda v+i\omega}\right]-\omega(\omega+i\gamma)$$
$$\times\left[\frac{B_-(e^{i\omega d/v}e^{-2Qd}-e^{-i\omega d/v})}{Qv-i\omega}\right.$$
$$\left.+\frac{B_+(e^{-i\omega d/v}e^{-2Qd}-e^{i\omega d/v})}{Qv+i\omega}\right]-\frac{C_-e^{i\omega d/v}}{Qv-i\omega}$$
$$\left.-\frac{C_+e^{-i\omega d/v}}{Qv+i\omega}\right\}. \tag{9}$$

Note that within the hydrodynamical approach, the only channel of energy dissipation is the excitation of surface and bulk plasmons. The momentum threshold of plasmon excitation is given by

$$\omega_p(q)=(\omega_p^2+\beta^2q^2)^{1/2}=qv, \tag{10}$$

which has only one solution if $v>\beta$, namely, $q_t=\omega_p/(v^2-\beta^2)^{1/2}$, and none if $v\leqslant\beta$. When $v>\beta$ the projectile can excite all plasmons of momentum $q>q_t$, leading to a divergent stopping. This divergence is removed if one considers the creation of electron-hole pairs. They can be implemented through a $q^2/2$ term in the dispersion curve of Eq. (10). This dispersion term describes the kinetic energy exchanged in binary collisions [24]. The nonlinear formalism used in Ref. [9] accounts for this term in $\epsilon(q,\omega)$ since spatial variations on the electron density are included in the internal kinetic energy per electron of the noninteracting Fermi gas. A more sophisticated electronic excitation spectrum of the medium is provided by the RPA dielectric function, which was first reported by Lindhard [25]. In what follows, we will describe the bulk properties via the RPA together with the Mermin prescription [26] (this will be

called the Mermin dielectric function below) in order to introduce a finite plasmon lifetime preserving the local particle number.

B. Local response approach

Many properties of the dielectric response of the interfaces can be analyzed by considering frequency-dependent response functions $\epsilon(\omega)$ of the bulk material. This is a very crude approximation that gives realistic results only when the external charge moves with very high velocities ($v \gg v_F$) or for points far away from the interface. This is the case, for instance, in scanning transmission electron microscopy, where the fast probe electrons have velocities of the order of half the speed of light. In spite of its simplicity, this approach reproduces the limits of the energy loss and loss probability for large velocity.

Solving the Poisson equation for the geometrical configuration of Fig. 1, one finds that the loss probability can be separated into bulk and surface contributions. The former reads

$$P_{bulk}(\omega)=\frac{aZ_1^2}{\pi v^2}\mathrm{Im}\left[\frac{-1}{\epsilon(\omega)}\right]\ln\left[\frac{\omega^2+q_c^2v^2}{\omega^2}\right],$$

which is nothing but the Bethe formula for the bulk loss probability. The hydrodynamic approach for the bulk dielectric constant yields the same result if $v \gg \beta$. Here q_c is the momentum cutoff that accounts for the minimum wavelength of the bulk polarization waves that the projectile can excite in the electron gas [27].

The surface loss probability can in turn be separated as

$$P_{surf}(\omega)=P_s(\omega)+P_{beg}(\omega)+P_i(\omega), \tag{11}$$

where

$$\begin{aligned}P_s(\omega)&=P_{s,1}(\omega)+P_{s,2}(\omega)\\&=\int dx\{S_1(Q,\omega)\mathrm{Im}[-G_{tf}(Q,\omega)]\\&\quad+S_2(Q,\omega)\mathrm{Im}[-g_s(\omega)]\},\end{aligned}$$

$$P_{beg}(\omega)=\mathrm{Im}\left[\frac{-1}{\epsilon(\omega)}\right]\int dxB(Q,\omega),$$

and

$$\begin{aligned}P_i(\omega)&=\mathrm{Im}[-g_s(\omega)]\mathrm{Im}\left[\frac{-1}{\epsilon(\omega)}\right]\\&\quad\times\int dxI(Q,\omega)\mathrm{Im}[-G_{tf}(Q,\omega)].\end{aligned}$$

In these equations,

$$\int dx=-4Z_1^2\int\frac{d\mathbf{Q}}{(2\pi)^2}\frac{2Qv^2}{[\omega^2+(Qv)^2]^2},$$

$$\begin{aligned}S_1(Q,\omega)&=\left(1+\mathrm{Re}\left[\frac{-1}{\epsilon(\omega)}\right]\right)\Big[(1+\mathrm{Re}[g_s(\omega)])\\&\quad\times e^{-Qa}\cos\left(\frac{\omega a}{v}\right)-\{1+\mathrm{Re}[g_s(\omega)]e^{-2Qa}\}\Big],\end{aligned}$$

$$\begin{aligned}S_2(Q,\omega)&=e^{-Qa}\mathrm{Re}[G_{tf}(Q,\omega)]\left(1+\mathrm{Re}\left[\frac{-1}{\epsilon(\omega)}\right]\right)\\&\quad\times\left[\cos\left(\frac{\omega a}{v}\right)-e^{-Qa}\right],\end{aligned}$$

$$\begin{aligned}B(Q,\omega)&=\mathrm{Re}[G_{tf}(Q,\omega)]\Big[1+\mathrm{Re}[g_s(\omega)]e^{-2Qa}\\&\quad-\{1+\mathrm{Re}[g_s(\omega)]\}e^{-Qa}\cos\left(\frac{\omega a}{v}\right)\Big],\end{aligned}$$

and

$$I(Q,\omega)=e^{-Qa}\left[\cos\left(\frac{\omega a}{v}\right)-e^{-Qa}\right],$$

where $g_s(\omega)=[1-\epsilon(\omega)]/[1+\epsilon(\omega)]$ is the local surface response function of the semi-infinite medium and

$$G_{tf}(Q,\omega)=\frac{g_s(\omega)(1-e^{-2Qa})}{1-g_s(\omega)^2e^{-2Qa}}$$

is the local surface response function of the slab. P_s is the contribution of the loss probability coming from the slab surface modes

$$\Omega_{s,\pm}=\omega_s[1\pm e^{-Qa}]^{1/2},$$

P_{beg} is the well-known *begrenzung* effect, which lowers the bulk energy loss, and P_i is the interference term between all bulk and surface modes. The surface effect for infinite thickness reduces to

$$P_{surf}(\omega)=\frac{-Z_1^2}{\omega v}\mathrm{Im}\left[\left(1-\frac{1}{\epsilon(\omega)}\right)g_s(\omega)\right].$$

Assuming a Drude-like bulk optical response [i.e., Eq. (4) with $\beta=0$] with zero damping, one finds

$$P_s(\Omega_\pm)=\frac{Z_1^2\pi}{2v}\left[1\mp\cos\left(2\pi\frac{a}{\lambda_s}\right)\right]$$

and

$$P_{beg}(\omega_p)=\frac{-Z_1^2\pi}{2v},$$

where $\lambda_s=2\pi v/\omega_s$ is the surface screening length. This quantity gives the range of distances in which the charged projectile is screened by the valence electrons of the medium. Notice the complementarity in P_s: the contribution of the Ω_+ (Ω_-) mode vanishes when the thickness is an even (odd) number of times $\lambda_s/2$. Hence the surface energy loss for infinite thickness reads

$$\Delta E_{\infty}=Z_1^2\frac{\pi}{v}\left(\omega_s-\frac{\omega_p}{2}\right)=\Delta E_{vac}^{in}+\Delta E_{sol}+\Delta E_{vac}^{out}, \quad (12)$$

where

$$\Delta E_{vac}^{in}=-Z_1^2\frac{\pi\omega_s}{4v}$$

is the energy gained by the projectile due to the image acceleration,

$$\Delta E_{sol}=Z_1^2\frac{\pi}{2v}(\omega_s-\omega_p)$$

is the energy lost due to surface plasmon excitation and begrenzung effects during the crossing part of the trajectory, and

$$\Delta E_{vac}^{out}=Z_1^2\frac{3\pi\omega_s}{4v}$$

is the energy lost during the outgoing part of the trajectory. The total effect always shifts up the energy, although it turns out to be negligible in comparison to the bulk energy loss for $a>\lambda_s$.

III. CONVOLUTION FORMULA FOR THE PROBABILITY DISTRIBUTION

This section is devoted to the derivation of the equation that governs the energy-loss distribution when both bulk and surface losses are present. Let $I(E,z)$ be the probability distribution of energy loss E at the position z. After traveling an infinitesimal distance dz the probability that the charge loses energy E' is given by $P(E',z)dz$ [this $P(E',z)$ is related to that of Eq. (5) by a factor of $1/v$, keeping in mind that $t=t(z)$], so that the distribution of scattered particles is given by $I_{loss}(E,z)dz$, where

$$I_{loss}(E,z)=\int_{-\infty}^{\infty}dE'I(E+E',z)P(E',z).$$

Moreover, the total number of scattered particles has to be subtracted from the distribution at the position z. This quantity is just the integral of I_{loss} over energy E. Then the evolution of the energy distribution is given by the kinetic equation

$$\frac{dI(E,z)}{dz}=-\frac{I(E,z)}{\lambda(z)}+I_{loss}(E,z), \quad (13)$$

where

$$\frac{1}{\lambda(z)}=\int_0^{\infty}dEP(E,z).$$

When taking $P(E)=P_{bulk}(E)$, λ becomes the mean free path associated with electronic excitations in the bulk divided by the thickness of the slab a. Equation (13) is a generalization of the well-known Bothe-Landau formula for the case of inhomogeneous media such as surfaces. Going over to Fourier space in the E dependence in Eq. (13) (the conjugate variable of E will be k) and integrating over z, one obtains [28]

$$I(E,z)=\int dke^{ikE}I(k,-\infty)e^{-N\Sigma(k,z)}, \quad (14)$$

with

$$\Sigma(k,z)=\int_{-\infty}^{z}dz'\sigma(k,z'),$$

where $\sigma(k,z)$ is the so-called transport cross section generalized to the case in which the loss probability is not independent of space and N is the density (atoms per volume) of the material. This transport cross section is related to the loss probability as

$$N\sigma(k,z)=\int dEP(E,z)(1-e^{ikE})$$
$$=2\pi[P(0,z)-P(-k,z)].$$

When $P(E,z)=P(E)$, $\Sigma(k,z)=z\sigma(k)$ and the standard Bothe-Landau formula is recovered. Equation (14) permits following the evolution of the probability distribution step by step as the projectile approaches, crosses, and leaves the medium, whatever the trajectory is (grazing incidence or crossing trajectory). For projectiles crossing a finite slab of thickness a, the probability distribution at the detector ($z=\infty$) is given by

$$I(E,z\to\infty;a)=\int dkI(k,-\infty)e^{iEk}e^{-2\pi[P(0)-P(-k)]},$$

where $P(E)=P_{bulk}(E)+P_{surf}(E)$. Assuming a Gaussian-like initial incident beam, the loss probability distribution takes the form

$$I(E,z\to\infty;a)=\int\frac{dk}{2\pi}e^{ik(E-E_{kin})}$$
$$\times e^{-\Delta E_{kin}^2k^2/8}e^{-2\pi[P(0)-P(-k)]}, \quad (15)$$

where E_{kin} and ΔE_{kin} are the incident kinetic energy and the beam-width, respectively.

In the diffusion approximation [13] the Fourier transform of the transport cross section $\sigma(k)$ is expanded up to second order in k and thus provides the Gaussian limit for the loss spectrum valid for large traveled thicknesses. According to this approximation one finds

$$I(E,z\to\infty;a\to\infty)=\sqrt{\frac{2}{\pi}}\frac{\exp\left(-2\frac{(-E+E_{kin}-aS)^2}{4aQ+(\Delta E_{kin})^2}\right)}{\sqrt{4aQ+(\Delta E_{kin})^2}}, \quad (16)$$

where $S=\Delta E/a$ is the stopping power and $Q=(1/a)\int d\omega\omega^2P(\omega)$ is the straggling.

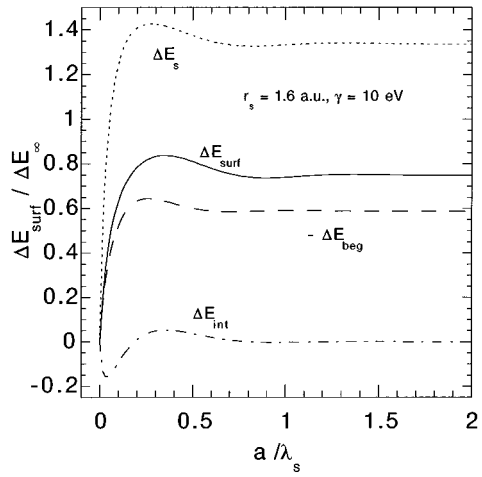

FIG. 2. Different contributions to the surface energy loss ΔE_{surf} of protons crossing a finite foil depicted as a function of the slab thickness scaled with the surface screening length λ_s within the local approach. The total surface energy loss (continuous line) can be separated into three terms [see Eq. (11)]: (i) the contribution of surface modes (dotted line), (ii) begrenzung (dashed line), and (iii) interference between surface and bulk modes (dash-dotted line). The material is amorphous carbon parametrized with $r_s=1.6$ a.u. and $\gamma=10$ eV. The results are scaled with the limit of infinite thickness ΔE_∞ [see Eq. (12)].

IV. RESULTS AND DISCUSSION

The different contributions within the local approach to the surface energy loss experienced by protons transmitted through an amorphous carbon foil ($r_s=1.6$ a.u. and $\gamma=10$ eV) are shown in Fig. 2 as a function of the slab thickness scaled with the surface screening length. The energy loss scaled with the limiting value of infinite thickness ΔE_∞ [Eq. (12)] presents no dependence on the velocity within this approach and only on the ratio between the slab thickness and the surface screening length a/λ_s and between the electron damping rate and the surface plasma frequency γ/ω_s. The surface energy loss shows oscillations with wavelength $\sim\lambda_s$, while the begrenzung effect oscillates with $\sim\lambda_p$. In practice the surface energy loss approaches the infinite thickness limit when $a\sim\lambda_s$, so that the two surfaces of the slab cannot ''see'' each other. The same behavior can be observed in the induced potential: for $a\geqslant\lambda_s$, the wake potential takes nearly the bulk limit for points inside the solid [8]. Although the main features are given by the pure surface term together with the begrenzung, the interference existing between bulk and surface collective modes also contributes when $a<\lambda_s$. Notice that the limit of large thickness lies below the value given by Eq. (12) due to the effect of damping.

In Fig. 3 the total energy loss experienced by protons crossing a finite medium slab due to the excitation of surface plasmons is depicted for several media and several velocities as a function of the slab thickness for the hydrodynamical model and it is compared with the results given using a local approach. The spatial dispersion makes the wavelength of the oscillations greater than λ_s and lowers the surface effect with respect to the value given by the local response. Even for $v=5$ a.u. the results given by the local approach are not

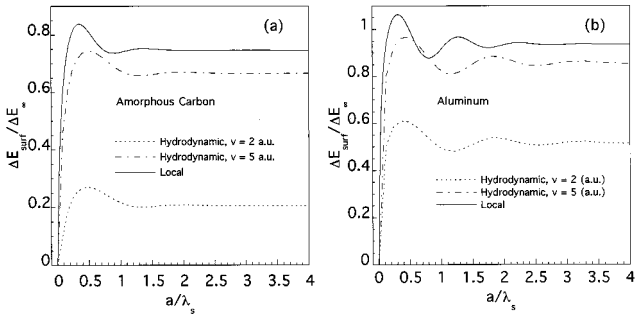

FIG. 3. Surface energy loss ΔE_{surf} experienced by protons crossing a finite foil represented as a function of the slab thickness scaled with the surface screening length λ_s within both local and hydrodynamical approaches [see Eq. (11) and Eqs. (8) and (9), respectively] for (a) amorphous carbon ($r_s=1.6$ a.u. and $\gamma=10$ eV) and (b) aluminum ($r_s=2.07$ a.u. and $\gamma=1.35$ eV). Different velocities have been considered. The values of the surface screening length are $\lambda_s=20.77$ and 52 a.u. in (a) and 30.56 and 70.4 a.u. in (b) for $v=2$ and $v=5$ a.u., respectively. The values of ΔE_∞ are $\Delta E_\infty=0.278$ and 0.111 a.u. in (a) and 0.189 and 0.077 a.u. in (b) for $v=2$ and 5 a.u., respectively.

achieved when dispersion is considered. The larger the electron damping, the more attenuated the oscillations.

The percentage of the surface effect with respect to the total loss as a function of the thickness of the slab can be seen in Fig. 4. The bulk energy loss has been calculated using the Mermin dielectric function in Eqs. (6) and (7) and the surface contribution within the hydrodynamical approach. The dependence on the velocity is only relevant for

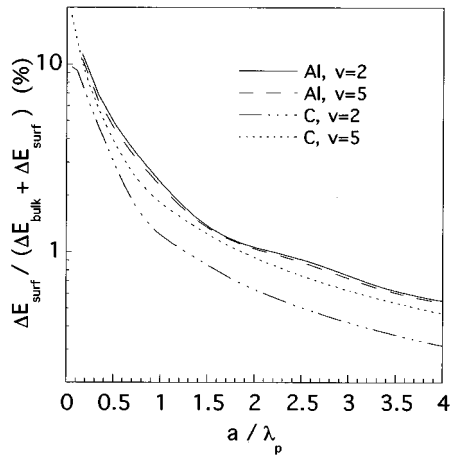

FIG. 4. Percentage of the surface energy loss with respect to the total energy loss $\Delta E_{surf}/\Delta E$ (%) represented for several r_s values and different velocities as a function of the slab thickness scaled with the bulk screening distance λ_p. The bulk energy loss has been calculated assuming the Mermin dielectric function [see Eqs. (6) and (7)], while the surface effect is calculated within the hydrodynamical approach [see Eqs. (8) and (9)]. The values of the bulk screening lengths are $\lambda_p=14.68$ and 36.71 a.u. for amorphous carbon ($r_s=1.6$ a.u. and $\gamma=10$ eV) and 21.61 and 54.02 a.u. for aluminum ($r_s=2.07$ a.u. and $\gamma=1.35$ eV) for $v=2$ and 5 a.u., respectively. The values of the bulk stopping power for protons are $S=0.307$ and 0.107 a.u. for amorphous carbon and 0.204 and 0.056 a.u. for aluminum for $v=2$ and 5 a.u., respectively.

materials with large damping electron rates, as in the case of amorphous carbon. Notice that the relative value of the energy loss drops to around 1% for $a \sim 2\lambda_p$.

Figure 5 shows the surface loss probability $P_{surf}(\omega)$ of protons crossing an amorphous carbon foil as a function of the energy transfer ω for different slab thicknesses and different approaches to the medium response. The dispersion effects considered via the hydrodynamical approach lower both the surface plasmon and the begrenzung bulk plasmon peaks and shift up their energy position with respect to the local approach. Even at $v=5$ a.u. the nonlocal dispersion effect is not negligible. The surface loss probability hardly depends on the foil thickness for $a>\lambda_p$ and only for $\omega \to 0$ can the difference be observed. For $a>\lambda_p$ the result obtained within the specular reflection model [21] is recovered, except for the limit of vanishing ω. For a fixed energy transfer ω, the probability shows oscillations of very small amplitude with the thickness. A finite damping results in a nonvanishing loss probability for $\omega=0$. For infinite thickness one has

$$P_{surf}(\omega=0)=\frac{3\pi\gamma}{2v\omega_s},$$

whereas for finite thickness $P_{surf}(0)$ diverges. The total energy loss is of course finite.

The inclusion of the surface loss probability in the total loss probability introduces two major effects for small thickness: (i) there is a nonzero probability at $\omega=0$ and (ii) the position of the maximum is shifted towards lower energies. This energy shift is due to the contribution of both the surface plasmon peak and the begrenzung. The latter also lowers the bulk plasmon peak. This is illustrated in Fig. 6.

In Fig. 7, the energy-loss spectrum I of 100-keV protons crossing a carbon foil is represented for several penetration lengths. Using the Mermin dielectric function in $P_{bulk}(\omega)$, the mean free path at $v=2$ a.u. is found to be $\lambda=4.5$ a.u., the bulk screening length for amorphous carbon being $\lambda_p=14.68$ a.u. The surface effect is negligible for thicknesses larger than λ_p. The relative height between the no-loss peak and the first plasmon-loss peak is lowered when the surface is considered. Only the peaks corresponding to one and two plasmon losses are clearly resolved when they are formed during the first stages of the penetration and the subsequent higher-order plasmon peaks cannot be distinguished anymore. All of them contribute to the straggling of the spectra. This could be applied to experimental situations in which a resonant process can take place when the projectile velocity is tuned via the energy-loss processes at a certain distance from the surface [29].

The dependence on the carbon slab thickness of the energy-loss spectrum of 100-keV protons is illustrated in Fig. 8. Little differences are found between the results given by the full calculation and the diffusion approximation: both the height and the energy position of the maxima do not coincide for small thickness. The diffusion approximation yields Gaussian spectra whose peaks correspond to the mean energy loss of the loss spectra and only when the Gaussian limit is achieved for larger thicknesses does the energy shift between both peaks and the difference in height become zero.

In Fig. 9 the experimental results reported by Matsunami [30] for 100-keV ($v=2$ a.u.) protons transmitted through a carbon foil of $a=120$ a.u. are compared with theory. All the calculated spectra account only for the bulk energy loss using the Mermin dielectric function since the surface effect for this thickness is negligible. In the diffusion approximation given by Eq. (16) we have used the calculated parameters $S=0.307$ a.u. and $Q=0.726$ a.u. The carbon foil has been simulated with $r_s=1.6$ a.u. and $\gamma=10$ eV. If one admits a Gaussian fluctuation of the slab thickness, the spectrum can be convoluted with the function

$$E_a(L)=\frac{1}{(2\pi)^{1/2}}\frac{\exp\left[-\frac{1}{2}\left(\frac{L-a}{\Delta L}\right)^2\right]}{\Delta L} \tag{17}$$

so that the loss spectrum is given by

$$I_a(E)=\int dL I(E,z\to\infty;L)E_a(L).$$

The main differences between the diffusion approximation and the full calculated spectra are found in the position of their respective energy peaks. The full calculation peak occurs at the position of the maximum of the spectrum E_p (most probable energy loss), while the diffusion approximation peak occurs at the theoretical mean energy loss ΔE. An energy shift $\delta=\Delta E-Ep$ of approximately 2 a.u. is found. This result agrees with previous reported experimental data [31]. As can be observed in Fig. 8, even for $a=120$ a.u. the loss spectrum does not achieve completely the Gaussian limit and thus the peak energy loss and the mean energy loss

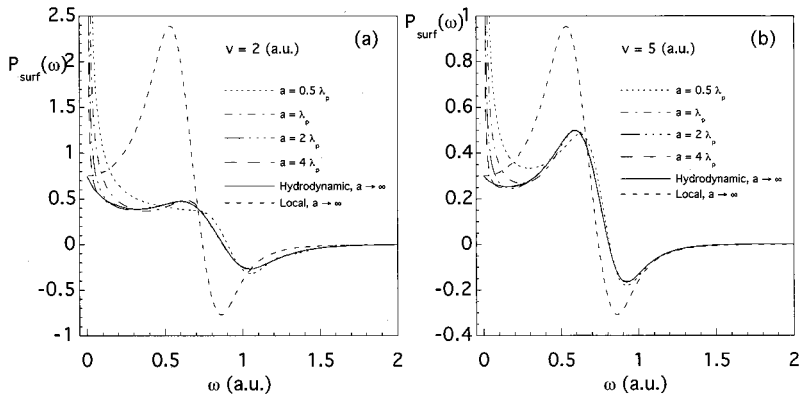

FIG. 5. Surface loss probability $P_{surf}(\omega)$ of protons crossing a finite foil of amorphous carbon ($r_s=1.6$ and $\gamma=10$ eV) depicted as a function of the energy transfer ω for several slab thicknesses within the hydrodynamical approach for (a) $v=2$ a.u. and (b) $v=5$ a.u. The continuous and dashed lines show the result of infinite thickness for the hydrodynamical and local approaches, respectively.

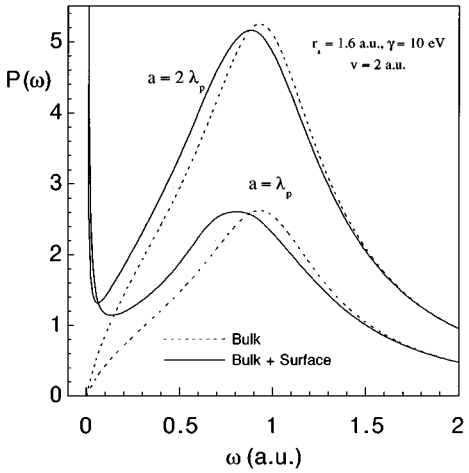

FIG. 6. Loss probability $P(\omega)$ of 100-keV protons ($v=2$ a.u.) crossing a finite slab of amorphous carbon ($r_s=1.6$ a.u. and $\gamma=10$ eV) with thickness $a=\lambda_p$ and $a=2\lambda_p$ as a function of the energy transfer ω. The dotted line represents the bulk loss probability $P_{bulk}(\omega)$ and the continuous line stands for the total loss probability $P_{bulk}(\omega)+P_{surf}(\omega)$. $P_{bulk}(\omega)$ [see Eqs. (6) and (7)] has been calculated using the Mermin dielectric function, while $P_{surf}(\omega)$ has been obtained within the hydrodynamical model [see Eqs. (8) and (9)].

do not coincide. Although the full calculation of $I(E,z\rightarrow\infty;a)$ shows a non-Gaussian shape that agrees better than the diffusion approximation with experiment, it does not account for the tail of large energy loss. A fluctuation of 10% in the determination of the slab thickness does not give a very different behavior.

Among the possible explanations for the discrepancy between this theory and the experiment for high-energy losses,

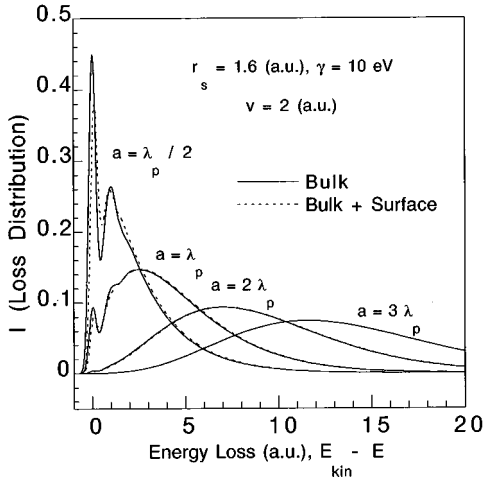

FIG. 7. Energy-loss spectra $I(E,z\rightarrow\infty;a)$ [see Eq. (15)] of 100-keV protons ($v=2$ a.u.) crossing a finite amorphous carbon slab ($r_s=1.6$ a.u. and $\gamma=10$ eV) for different penetrated thicknesses. The Mermin dielectric function has been used to calculate the bulk losses (continuous line) and the hydrodynamical model to include surface effects (dotted line). Using the Mermin approximation, the mean free path is found to be $\lambda=4.5$ a.u. The bulk screening length is $\lambda_p=14.68$ a.u. The spectra have been normalized to unity. The beam width has been chosen as $\Delta E_{kin}=10^{-4}E_{kin}$.

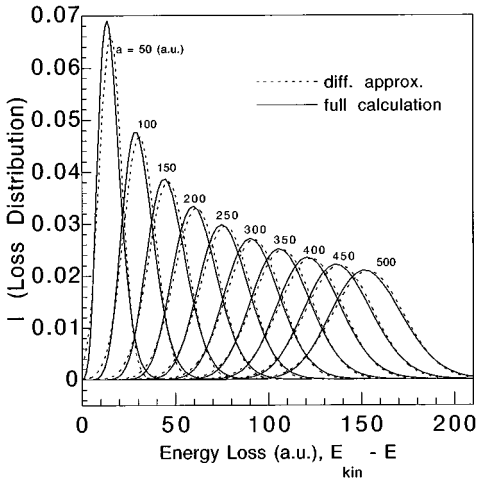

FIG. 8. Energy-loss spectra $I(E,z\rightarrow\infty;a)$ of 100-keV protons ($v=2$ a.u.) crossing finite amorphous carbon slabs ($r_s=1.6$ and $\gamma=10$ eV) of different thickness (labeled at every curve). The continuous line represents the full calculation of the spectra [see Eq. (15)] and the dotted line represents the diffusion approximation [see Eq. (16)]. The Mermin dielectric function has been used to calculate the loss probability function $P(E)$ [see Eq. (7)] in both cases. The calculated stopping power and straggling used as parameters in the diffusion approximation are $S=0.307$ a.u. and $Q=0.726$ a.u., respectively. The spectra have been normalized to unity. The beam width has been chosen as $\Delta E_{kin}=10^{-4}E_{kin}$.

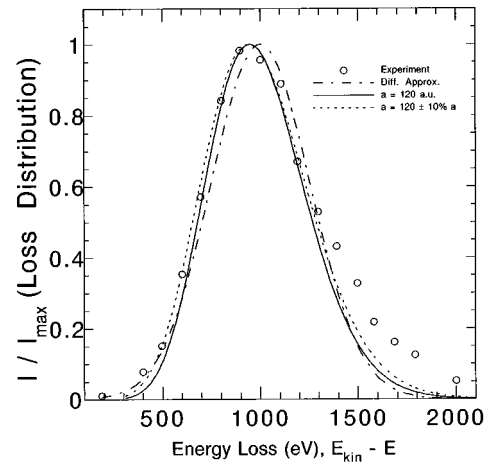

FIG. 9. Energy-loss spectrum $I(E,z\rightarrow\infty;a)$ for 100-keV protons transmitted through a carbon foil ($r_s=1.6$ a.u. and $\gamma=10$ eV) with thickness $a=120$ a.u. The open circles represent the experimental data reported by Matsunami [30], the dash-dotted line shows the spectrum given within the diffusion approximation [Eq. (16)], the continuous line shows the full calculated spectrum [Eq. (15)], and the dashed line shows the same spectrum as the continuous one but taking into account a Gaussian error with $\Delta a=\pm 12$ a.u. in the thickness of the carbon foil [see Eq. (17)]. Only the bulk contribution to the spectrum has been considered in $P(E)$ [see Eq. (7)] using the Mermin dielectric function. The calculated stopping power and straggling are $S=0.307$ a.u. and $Q=0.726$ a.u., respectively. The spectra have been scaled with their maximum value. The beam width has been chosen as $\Delta E_{kin}=10^{-4}E_{kin}$.

one has to consider that the solid has been modeled by a free-electron gas, neglecting in this way large energy losses that could take place due to the localization of the solid electrons (even those of the valence band). Inner shells can be ruled out since the ionization of the K shell of carbon, calculated within the first Born approximation using a Hartree-Fock-Slater model potential and taking the electron binding energies and wave functions as those of the isolated carbon atom [32], results in a contribution to the stopping power of $S_{1s}=8.52\times10^{-3}$ a.u. for $v=2$ a.u., which gives only 3% of the total energy loss.

V. SUMMARY

The effect of the surface in the energy loss of ions passing through thin films has been studied using both a hydrodynamical approach and a local-response picture. The inclusion of the spatial dispersion in the collective electronic modes lowers the surface energy loss with respect to the local result, but does not change it qualitatively.

A convolution formula that contemplates the scattering due to the surface is used beyond the diffusion approximation to show non-Gaussian loss spectra with and without inclusion of surface effects. A comparison with experiments results in better agreement with respect to the diffusion approximation, although it does not account for the tail of large energy loss taking place in the experimental spectrum. This discrepancy is possibly due to the fact that the free-electron-gas model does not account for large energy losses that could take place due to the localization of the solid electrons.

The effect of the surface can be observed only for foil thicknesses smaller than or of the order of the screening length $2\pi v/\omega_s$, which is in the range 10–30 Å for protons moving with 100–1000 keV. The relative value of the surface energy loss with respect to the total energy loss drops to around 1% for these thicknesses and below this range the surface screening properties are not efficiently fulfilled.

ACKNOWLEDGMENTS

The present work has been supported by the Spanish Ministerio de Educacion y Ciencia, the Basque Government (Eusko Jaurlaritza), and Iberdrola S.A.

[1] R. H. Ritchie, Phys. Rev. **106**, 874 (1957).
[2] N. Takimoto, Phys. Rev. **146**, 366 (1966).
[3] M. Sunjic and A. A. Lucas, Phys. Rev. B **3**, 719 (1971).
[4] E. Wikborg and J. E. Inglesfield, Phys. Scr. **15**, 37 (1977).
[5] Z. Penzar and M. Sunjic, Phys. Scr. **30**, 453 (1984).
[6] P. Feibelman, Phys. Rev. B **9**, 5077 (1974).
[7] Godfrey Gumbs and Norman J. M. Horing, Phys. Rev. B **43**, 2119 (1991).
[8] F. J. García de Abajo and P. M. Echenique, Phys. Rev. B **45**, 8771 (1992).
[9] José J. Dorado, Oakley H. Crawford, and Fernando Flores, Nucl. Instrum. Methods Phys. Res. B **93**, 175 (1994).
[10] S. P. Apell, John R. Sabin, and S. B. Trickey, Int. J. Quantum Chem. **S29**, 153 (1996).
[11] N. Bohr, Philos. Mag. **25**, 10 (1913).
[12] L. Landau, J. Phys. (Moscow) **8**, 201 (1944).
[13] P. Sigmund, in *Interaction of Charged Particles with Solids and Surfaces*, Vol. 271 of *NATO Advanced Study Institute, Series B: Physics*, edited by A. Gras-Marti *et al.* (Plenum, New York, 1991), p. 73.
[14] P. Sigmund, Nucl. Instrum. Methods Phys. Res. B **69**, 113 (1992).
[15] A. Närmann and P. Sigmund, Phys. Rev. A **49**, 4709 (1994).
[16] Y. H. Ohtsuki, T. O'hori, and R. Kawai, Nucl. Instrum. Methods Phys. Res. B **194**, 35 (1982); T. O'hori and Y. H. Ohtsuki, Phys. Rev. B **27**, 3418 (1983).
[17] K. Kimura, M. Hasegawa, Y. Fujii, M. Suzuki, Y. Susuki, and M. Mannami, Nucl. Instrum. Methods Phys. Res. B **33**, 358 (1988).
[18] T. Iitaka, Y. H. Ohtsuki, A. Koyama, and H. Ishikawa, Phys. Rev. Lett. **65**, 3160 (1990).
[19] F. Bloch, Z. Phys. **81**, 363 (1933); Helv. Phys. Acta **7**, 385 (1934).
[20] R. H. Ritchie and A. L. Marusak, Surf. Sci. **4**, 234 (1966).
[21] F. J. García de Abajo and P. M. Echenique, Phys. Rev. B **46**, 2663 (1992).
[22] P. M. Echenique, F. Flores, and R. H. Ritchie, Solid State Phys. **43**, 229 (1990).
[23] F. Flores and F. García Moliner, J. Phys. C **12**, 907 (1979).
[24] P. M. Echenique, F. J. García de Abajo, V. H. Ponce, and M. E. Uranga, Nucl. Instrum. Methods Phys. Res. B **96**, 583 (1995).
[25] J. Lindhard, Kg. Dan. Vidensk. Selsk. Mat. Fys. Medd. **28**, No. 8 (1954).
[26] N. D. Mermin, Phys. Rev. B **1**, 2362 (1970).
[27] P. M. Echenique, R. H. Ritchie, N. Barberán, and John Inkson, Phys. Rev. B **23**, 6486 (1981).
[28] The use of the Fourier transform instead of the Laplace transform as done by Landau allows the possibility of gaining energy.
[29] F. Javier Pérez Pérez, Isabel Abril, Néstor R. Arista, and Rafael García Molina, Nucl. Instrum. Methods Phys. Res. B **115**, 18 (1996).
[30] Noriaki Matsunami, Nucl. Instrum. Methods Phys. Res. B **115**, 14 (1996).
[31] Noriaki Matsunami and Kenshin Kitoh, Nucl. Instrum. Methods Phys. Res. B **59**, 5 (1991).
[32] J. I. Juaristi, F. J. García de Abajo, and P. M. Echenique, Phys. Rev. B **53**, 13 839 (1996), and references therein.